Behavior of Ionically Charged Lamellar Systems under the Influence of a Shear Field

M. Bergmeier,[†] M. Gradzielski,*[,†] H. Hoffmann,[†] and K. Mortensen[‡]

Lehrstuhl für Physikalische Chemie I, Universität Bayreuth, D-95440 Bayreuth, Germany, and Condensed Matter Physics and Chemistry Department, Risø National Laboratory, DK-4000 Roskilde, Denmark

Received: August 25, 1998; In Final Form: December 7, 1998

The influence of a shear field on differently charged bilayers is studied by means of rheology, anisotropy of the electrical conductivity, freeze−fracture transmission electron microscopy, and small-angle neutron scattering (SANS). The charge density in the aqueous system tetradecyldimethylamineoxide (TDMAO)/tetradecyltrimethylammonium bromide (TTABr)/*n*-hexanol was varied by changing the content of TTABr from 0 to 10 mol %. At low TTABr content, preferentially planar lamellae are formed, and at higher TTABr content, multilamellar, polydisperse vesicles (1 μm and larger), which are densely packed and therefore possess elastic properties and a yield stress value. It is shown that the effect of the shear field is such that at first the planar lamellae are transformed into vesicles. Once multilamellar vesicles are present, further increase of the shear rate causes vesicle shells to be stripped off until, at high shear rates, unilamellar vesicles are formed. This leads to an increase of the elastic properties and the yield stress value. The formed unilamellar vesicle system is found to be stable and does not relax back into its original state. Thus shearing is prooved to be a suitable method for control of the morphology of vesicles. The results can be rationalized in terms of the bending elasticity of the bilayer and the position of the investigated sample in the phase diagram.

I. Introduction

Vesicles have recently become a fascinating subject in surfactant science. They fulfill basic functions in physiological systems as bilayer lipid membranes and thus represent model systems for biologigal membranes.[1,2] Vesicles are applied in pharmaceutics, where they are used as drug delivery systems. For example, anthracyclines (active agents against cancer) can be encapsulated within vesicles and thus improve the therapeutic effectiveness.[3] Vesicles may occur in different states, such as unilamellar or multilamellar vesicles, and their degree of polydispersity can vary widely.

Originally, vesicles were mainly formed by methods such as ultrasonification or the microfluidization technique,[4] but by now, many surfactant systems are known in which they form spontaneously.[5−8] In general, a tendency for the transformation of a conventional lamellar phase into the vesicle state is to be expected for the case of charging up the amphiphilic membrane.[9]

Roux et al.[10,11] have shown that technological handling and size control of vesicles is possible by exposing the vesicle phases to different shear rates. They established so-called shear diagrams describing the different shear rate regimes of lamellar phases. At low shear rates, they found defective lamellar structures. At medium shear rates, these defective lamellar structures are transformed into vesicles. Their size is controlled by the shear rate in a way that with increasing shear rate a reduction of particle diameter is observed (it might be noted here that, for vesicles in the system dioctadecyldimethylammonium chloride/water, also a reduction of size by application of shear has been found).[12] Finally, at high shear rates, these vesicles are transformed back into lamellae, but now are defect free. Their work mainly dealt with semidilute surfactant solutions with interlamellar spacings in the range from 50 to a few hundreds of angstroms. For some cases, they found spherulitic lamellar phases containing foamlike vesicles of high monodispersity.[13] In the case of a fairly concentrated system, also formation of a close-packed assembly of multilayered vesicles has been observed under shear.[14]

In the last few years, the interest in vesicles and the effects of shear on them has grown enormously. Different methods have been employed to investigate shear-induced transformations, such as NMR,[15] stress-controlled rheology,[16] rheo small-angle light scattering,[17] SANS,[18] and the combined application of light and neutron scattering.[19,20] Schmidt et al. confirmed two of the shear-induced structures formerly described by Roux by their characteristic NMR line shapes.[15] While Roux found a mere rate dependence of vesicle parameters, Bergenholtz and Wagner[16] deduced a stress-controlled behavior of their model lamellar phase. Their system turned out to be extremely sensitive on the shear history. Richtering et al.[17,19,20] also found shear rate induced transitions that were reversible. The formation of vesicles needed a long time to take place and was accompanied by complex rheological behavior such as shear thickening. In their scattering experiments, they found butterfly patterns at high shear rates, which they ascribed to an assembly of vesicles disorderd in the direction of flow.

Mendes et al.[18] were able to show a new transition under shear from vesicles to wormlike micelles. They also observed long characteristic times for the shear-induced transitions. The importance of shear effects during the preparation of vesicle phases was shown by Hoffmann et al.[21] They found that without the presence of a shear field a stacked lamellar phase is formed when an L_3 phase from a zwitterionic surfactant becomes charged by protonation due to a hydrolysis reaction, while the same preparation with identical components and concentrations yields a vesicle phase with a yield stress if the shear is applied during the preparation.

The studies in this paper will now focus on a dilute model system with an overall surfactant concentration of only 100 mM and amazing macroscopic properties such as elasticity and a

[†] Universität Bayreuth.
[‡] Risø National Laboratory.

10.1021/jp983480d CCC: $18.00
Published on Web 02/17/1999

yield stress value. Shear experiments on a system that was charged by addition of 10 mol % of a cationic surfactant (TTABr) showed that the originally present multilamellar vesicles can become transformed into small unilamellar vesicles by the shear field.[22] In the following, we have studied this system in much more detail, especially with respect to the variation of the charge density of the amphiphilic bilayer, where the charge density is controlled by the mixing ratio of nonionic and cationic surfactant.

II. Materials and Methods

II.1. Materials. Tetradecyldimethylamine oxide (TDMAO) was a gift from Clariant (Gendorf) and was recrystallized twice from acetone before use. Tetradecyltrimethylammonium bromide (TTABr) was obtained from Fluka and was recrystallized twice from ether/ethanol (50/50 v/v). 1-Hexanol was also obtained from Fluka in purissimum quality. Water was deionized and double distilled before use. D_2O (99.9% isotopic purity) was obtained from Euriso-top, Groupe CEA, C. E. Saclay (Gif-sur-Yvette, France).

II.2. Methods. *II.2.1. SANS.* The small-angle neutron scattering experiments were performed at the SANS instrument at the Risø National Laboratory, where the scattering intensity was measured with a 2-D detector. For the static experiments, Hellma quartz cuvettes of 1 mm thickness were employed and a q range of 0.006−0.5 1/Å. The shear experiments were done in a Couette cell that has been described in detail before.[23] Absolute calibration and normalization to detector response was done by the standard method using the incoherent scattering from water as a secondary standard and taking into account the background counts from the detector, the scattering of the empty cell, and the transmission of the sample[24] (this was not done for the measurements in the Couette cell). In addition to the usual azimuthally averaged radial dependence of the scattering intensity, $I(q)$ (with $q = |\mathbf{q}|$), we also studied the azimuthally dependent intensities as averaged over the q interval of 0.01−0.015 1/Å around the peak value.

II.2.2. Rheological Measurements. The rheological measurements were performed with a Bohlin CS 10 rheometer. A double gap system was used to avoid evaporation effects. The lowest possible stress value amounts to 3 mPa. The viscoelastic properties were determined by oscillatory measurements from 0.001 to 10 Hz, whereby alternatively the strain amplitude or the stress amplitude can be kept constant. For measurements at higher shear rates, a Rheolab MC20 (Physica) was employed, which in principle operates in a manner similar to the Bohlin instrument. In all the shear experiments, the shear rate was controlled.

II.2.3. FF-TEM. For the freeze−fracture transmission electron microscopy (FF-TEM), a small amount of the sample was placed on a 0.1 mm thick copper disk covered with a second copper disk. The sandwich was frozen by plunging it into liquid propane, which was cooled by liquid nitrogen. Fracturing and replication were carried out in a BALZERS BAF 400 freeze−fracture apparatus at a temperature of −140 °C. Pt/C was deposited under an angle of 45°. The replicas were examined in a CEM 902 electron microscope (Zeiss, Germany).

II.2.4. Anisotropy of the Electrical Conductivity. The setup for the measurement of the electrical conductivity was homemade. We used a Searle-type gap system with the inner part rotating and the outer part static. The arrangement of the electrodes gives information about the conductivity in the different directions of space. This setup is displayed in Figure 1.

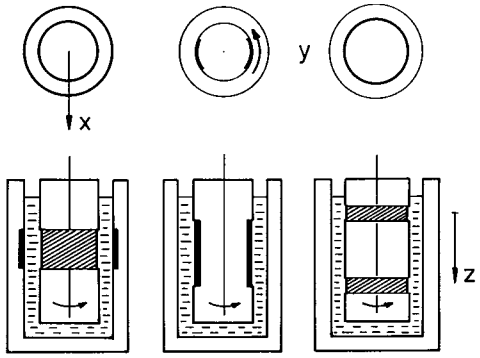

Figure 1. Schematic display of the Couette setup used for the measurement of the anisotropy of the electric conductivity. The axes x, y, and z defined here are used identically for the Couette setup of the SANS experiments, i.e., in the SANS experiments one detects in the $y-z$ plane; x is along the velocity gradient, y along the direction of shear, and z along the axis of vorticity.

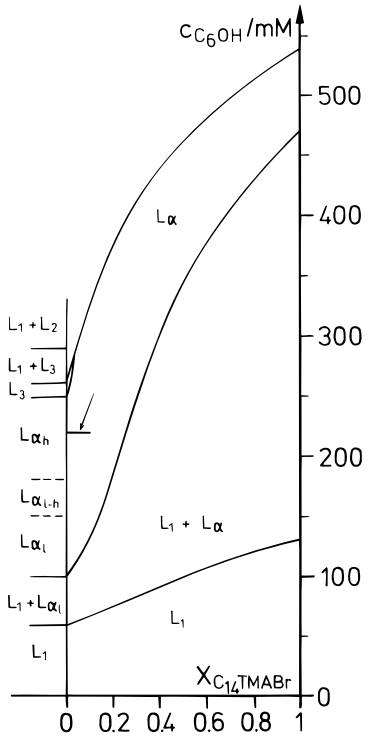

Figure 2. Schematic quaternary phase diagram of zwitterionic tetradecyldimethylamineoxide (TDMAO), cationic tetradecyltrimethylammonium bromide (TTABr), 1-hexanol, and water at 25 °C. The overall surfactant concentration is 100 mM. The ordinate to the very left of the phase diagram represents the phase sequence in the ternary system TDMAO/1-hexanol/water: L_1 = isotropic micellar solution; $L_{\alpha l}$ = vesicle phase (onion phase); $L_{\alpha h}$ = classical lamellar phase; L_3 = L_3 phase (sponge phase). The line of investigation at 220 mM 1-hexanol is indicated by an arrow.

All the experiments described in the following were done at 25 °C.

III. Results and Discussions

III.1. Phase Behavior at Rest. In our system, vesicles are easily formed by addition of the cationic surfactant tetradecyltrimethylammonium bromide (TTABr) to the ternary system tetradecyldimethylamineoxide TDMAO/1-hexanol/water (Figure 2).[25−28] The total surfactant concentration was always 100 mM, and different phases can be adjusted by variation of the content of the cosurfactant hexanol. The phase sequence in the ternary

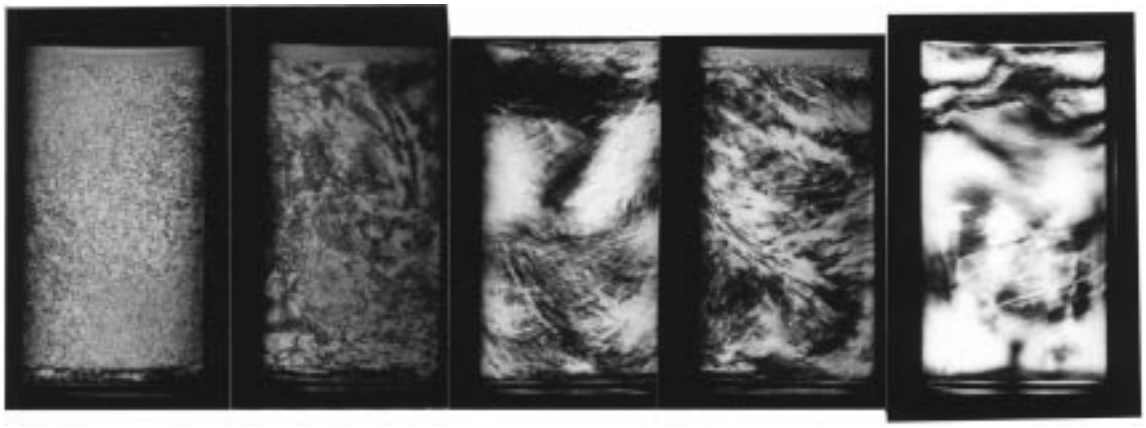

Figure 3. Samples of 100 mM (TDMAO/TTABr)/220 mM 1-hexanol/water photographed between crossed polarizers at different charge densities of the amphiphilic bilayer. The concentrations of ionic surfactant TTABr are 0, 0.25, 0.5, 1, and 10 mol % from left to right.

system (left side of Figure 2) is complex and several multiphase regions are formed. Upon addition of hexanol to the isotropic micellar solution (L_1),[29] the mean spontaneous curvature is lowered and the typical phase shift from micelles via vesicles and planar lamellae to the sponge phase (L_3) is observed. In the $L_{\alpha l}$ phase (at low cosurfactant concentration), vesicles are found, while at high cosurfactant concentration in the $L_{\alpha h}$ phase, planar lamellae are present. In between, both vesicles and lamellae are present ($L_{\alpha 1-h}$) (as evidenced from FF-TEM micrographs). The $L_{\alpha 1-h}$ phase can therefore be considered as a 2Φ region that does separate microscopically but not macroscopically.

Upon addition of the cationic surfactant, the phase diagram is drastically simplified. The L_3 phase is suppressed because the bilayer membrane is now charged. The different L_α phases now converge into a wide single L_α phase that is solely made up of vesicles.[30,31] This is also understood theoretically as the charges on the amphiphilic film render the Gaussian modulus negative and thereby reduce the stability of the L_3 phase and increase that of vesicles.[9,32] Also, the phase boundary between the L_1 phase and the vesicular L_α phase shifts to a higher cosurfactant concentration. This vesicular L_α phase is of special interest because of its microstructure that results in amazing rheological properties. It consists of densely packed multilamellar vesicles. The charged and stiffened bilayer gives rise to elastic properties and a yield stress value, i.e., air bubbles in a sample do not rise and the solution can be used as a suspending fluid. The moduli are mainly determined by electrostatic interaction, and upon addition of salt, a breakdown of the elastic properties has been observed.[28]

In the following, we will examine shear experiments on samples of different charge density of the amphiphilic bilayer. For that purpose, we studied systems of constant total composition where only the ratio of TTABr/TDMAO (i.e., the charge density) varies; that is, this corresponds to a horizontal line at 220 mM hexanol content in Figure 2. The content of TTABr in the surfactant mixture was varied in steps by choosing TTABr contents of 0, 0.25, 0.5, 1, 3, 5 and 10 mol %. Thus, we start from a purely lamellar phase that contains no vesicles. A sample of such a solution of pure TDMAO shows a typical domainlike birefringence pattern between crossed polarizers (very left in Figure 3). The sample containing 0.25 mol % TTABr already shows a stress-induced so-called schlieren texture, but is still exhibiting some domainlike birefringence. This domainlike birefringence pattern becomes weaker until at 0.5 and 1 mol % TTABr the stress-induced pattern is dominant. For 10 mol % TTABr, the birefringence pattern is exclusively stress induced. The domainlike birefringence pattern is due to the lamellar structure that is present in the solution, and its intensity corresponds to the amount of lamellae present. The charging process thus reduces the fraction of lamellae until, at around 3%, no more planar lamellae can be detected but only vesicles. This is to be expected because the Gaussian modulus becomes more and more negative with increasing charge density.[9]

To characterize more carefully this initial situation prior to any shear experiments, TEM pictures have been taken (Figure 4). Figure 4a shows a sample that contains 0.25 mol % TTABr. It displays the typical situation of a microscopic coexistence regime of planar lamellae and vesicles. The sample therefore is microscopically biphasic with clusters of vesicles next to extended planar bilayers. The vesicles are polydisperse in size. Some are deformed into elongated structures, and at the interface between vesicles and planar bilayers, even tubular particles can be observed. The planar lamellae are rippled and exhibit high flexibility. Though obviously a biphasic situation is displayed, no macroscopic phase separation takes place because the solution has a yield stress value that prevents the system from any diffusion or reorganization processes.

In Figure 4b, a solution with 1 mol % TTABr is displayed that contains mainly vesicles. On closer inspection of the micrograph, one finds, however, open-shell fragments and vesicles with nonclosed layers. These lamellar fragments cause the domainlike birefringence pattern observed between crossed polarizers. Thus, this solution can be considered a single-phase vesicle solution with defects.

At 3 mol % TTABr content (Figure 4c), a typical vesicle solution is displayed. The vesicles are very polydisperse in size (40 nm up to 2 μm or even larger) and densely packed. No more lamellar fragments are observed. The sufficiently high charge density for the formation of a pure vesicle solution seems to be reached. At a TTABr content of 10 mol % (Figure 4d), the typical onion phase is displayed; a system of densely packed, multilamellar vesicles with a high polydispersity in size and no lamellar fragments are found. The sample shows prevalently cross-fracturing, while the bilayers with small charge density have a tendency to fracture along the midplane of the bilayer. The way of fracturing gives a hint about the forces within the bilayer. Fracturing along the midplane of the bilayer indicates weak adhesion forces, while cross-fracturing is characteristic of strongly adhering bilayers. So the charging of the bilayer seems to reinforce the bilayer and increase its stability.

In the following investigations of the effect of shear on charged lamellar phases, the content of planar lamellae fragments has to be taken into account. Therefore, this paper is

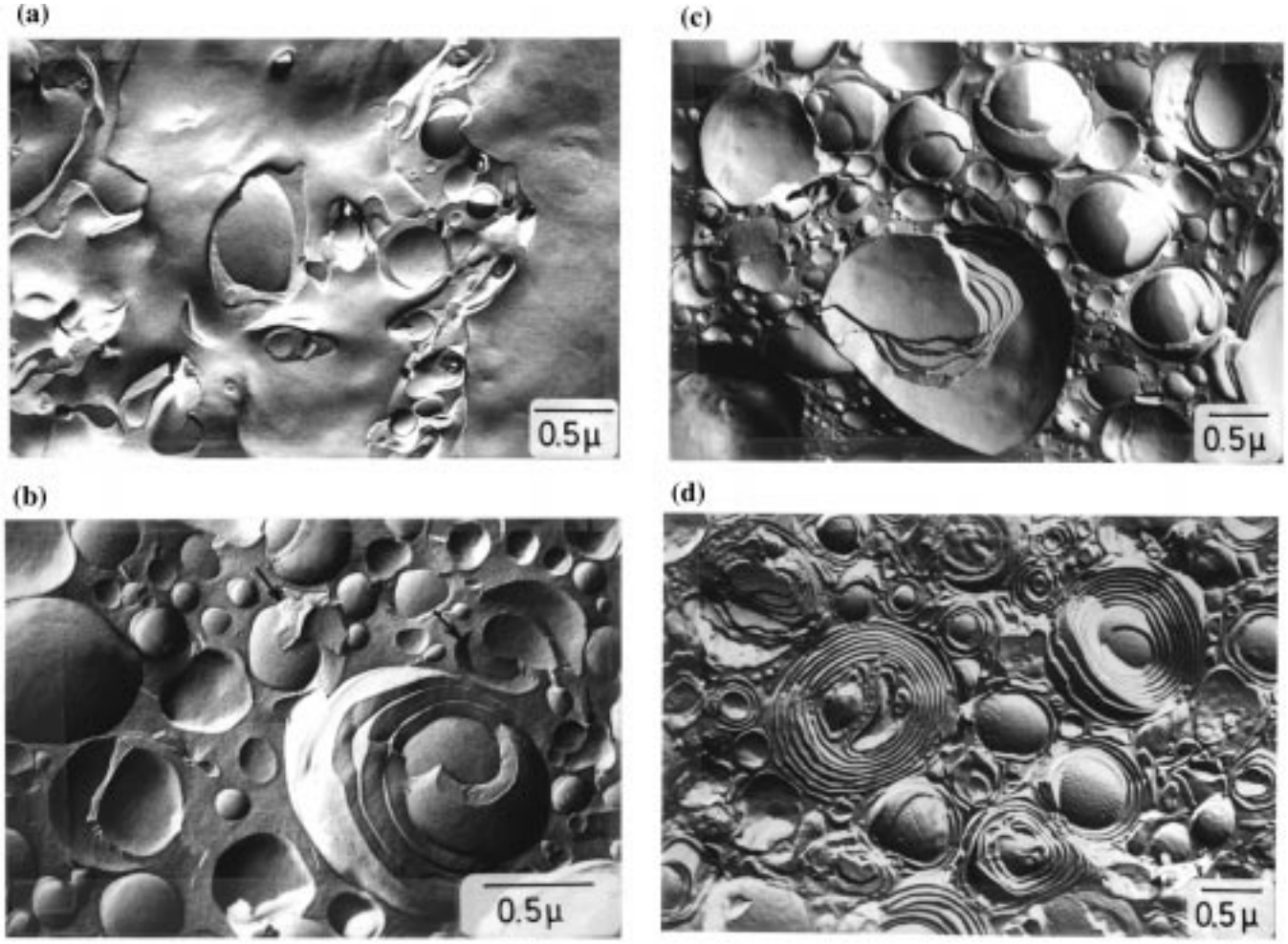

Figure 4. Freeze−fracture TEM micrographs of differently charged systems (see phase diagram Figure 1). The total surfactant concentration is 100 mM and the degree of charged surfactant is varied by adjusting the molar TTABr/TDMAO ratio: (a) 0.25 mol %; (b) 1 mol % (some of the open shell fragments have been marked with arrows); (c) 3 mol %; (d) 10 mol % TTABr.

divided into two further sections. Section 1 (III.2) deals with the onion phase, which is highly charged due to the presence of 10 mol % TTABr and contains no lamellar fragments. Section 2 (III.3) deals with phases of lower charge density (0.25, 0.5, 1 mol % TTABr), which contain both lamellar fragments and vesicles and show a more complex rheological behavior. It will be shown that this behavior can be ascribed to the transformation of lamellae into vesicles under shear.

III.2. Behavior Under Shear of the Onion Phase Containing 10 mol % TTABr. In the following, the behavior in the shear field of a sample of composition 90 mM TDMAO/10 mM TTABr/220 mM 1-hexanol (for the SANS measurements in D_2O) has been investigated in detail.

III.2.1. Electric Conductivity. Figure 5 shows a typical diagram of the conductivity under shear. By a simple Couette setup, it is both possible to shear a vesicle solution with shear gradients up to 2000 s^{-1} and measure the conductivity in different directions perpendicular and parallel to the shear gradient by a corresponding arrangement of electrodes.[33,34] The diagram shows the conductivity in vorticity direction perpendicular to the shear gradient of 2000 s^{-1}. The conductivity without shear is about 100 μS/cm, and upon shearing, it increases to a value of about 200 μS/cm. This value is constant under shear, and a steady state is reached where the observed conductivity increases with increasing applied shear rate (Figure 6).

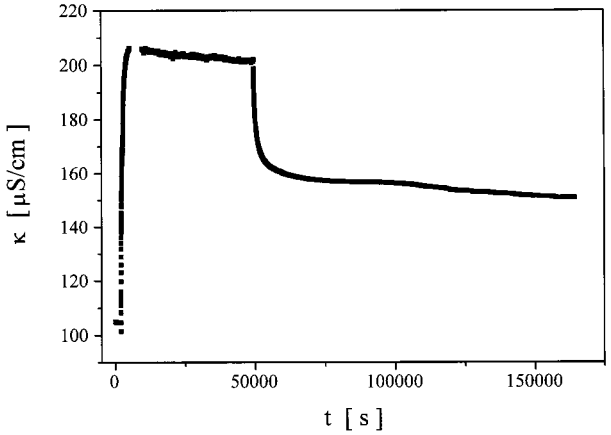

Figure 5. Plot of the specific conductivity (under shear as a function of the elapsed time frequency for the system 90 mM TDMAO/10 mM TTABr/220 mM hexanol. The applied shear rate was 2000 s^{-1} (the shear was turned on at $t = 0$ s and switched off at $t = 50\,000$ s).

After stopping the shear, the conductivity relaxes in a biexponential process (with a short time constant of 10 min and a long time constant of 2 h) until a value of about 150 μS/cm is reached, which remains constant (some slow decrease still takes place in the course of days). This means that within days the vesicle solution does not relax back to its original state, indicating that a long-time change has been imposed on the

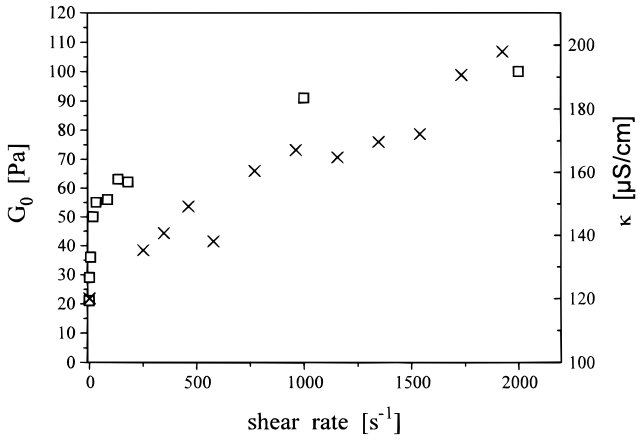

Figure 6. Plot of the shear modulus G_0 (□) and the electric conductivity κ (×) versus shear rate of the preshear for the system 90 mM TDMAO/10 mM TTABr/220 mM hexanol. The vesicle solution was sheared at a certain shear rate until the apparent shear viscosity indicated a steady state. Then, the shear was stopped and the modulus was measured in an oscillation experiment. The electric conductivity was measured in the vorticity direction during shear.

system. This conductivity behavior is typical for all directions, i.e., perpendicular and parallel to the shear gradient. The results may be explained by a reduction of vesicle shells due to the shear and the corresponding release of counterions. It has been shown before that it is possible to determine the number of vesicle shells by comparison of the conductivity value of the vesicle phase with the conductivity of a corresponding micellar solution.[26] The conductivity in a vesicle phase is low due to the encapsulation of counterions while it is much higher in the micellar solution where no counterions are entrapped. Thus, the ratio of the conductivity in the L_α phase to the conductivity in the L_1 phase is a measure of the number N of vesicle shells.[26]

$$\frac{\kappa}{\kappa_0} = \frac{N^2}{3\sum_{n=1}^{N} n^2} = \frac{2N}{(N+1)(2N+1)} \qquad (1)$$

κ and κ_0 are the conductivity in the L_α phase and the L_1 phase, respectively.

Applying this formula to our shear experiment shows that the vesicles sheared with a gradient of about 2000 s^{-1} should be unilamellar to a large degree. This is in accordance with the fact that the conductivity under shear is the same in all directions (whereas they are different at rest), since unilamellar vesicles are not easily deformed. Thus, no anisotropy of the conductivity can occur. After the shear is stopped, vesicle shells or lamellar fragments are partly reconstructed and the conductivity first decreases quickly but is then trapped at an intermediate value between the value under shear and the value prior to shear; that is, the final state is different from the original state.

III.2.2. Rheology. The vesicle solution at rest exhibits elastic properties and a yield stress of about 2 Pa. The rheological properties can be described by a classical Bingham gel; that is, the moduli are frequency independent. The storage modulus is around 20 Pa and always one decade higher than the loss modulus. It should be noted that the value of the storage modulus is very close to the one observed for densely packed unilamellar phospholipid vesicles of 250 nm radius.[35]

Shearing such a solution leads to a strong increase of the storage modulus and of the yield stress. Figure 6 shows the shear rate dependence of the storage modulus. Here, the solution was sheared at a certain shear rate until the on-line monitored apparent shear viscosity was constant (usually within 1−3 h). Then, the shear was stopped and the moduli were measured in an oscillation experiment. The higher the shear rate is, the higher the storage modulus G'. For the same type of experiment, also an increase of the conductivity under shear is observed with rising shear rate; that is, both conductivity and shear modulus show a similar behavior.

Such a behavior can be explained by the stripping off of vesicle shells, which leads to the buildup of new and smaller vesicles. Thus, the number density of vesicles is increased on cost of the average number of shells per vesicle. This increase of the number density ^1N of vesicles results in a higher storage modulus G_0, since it should be proportional to the number density of the particles present according to $G_0 \approx {}^1NkT$.[36,37]

III.2.3. Freeze−Fracture Transmission Electron Microscopy (FF-TEM). The effect of shear can be shown unambiguously by FF-TEM micrographs. Figure 4d shows a micrograph of the unsheared system. The vesicles are densely packed and very polydisperse in size. The size range is from very small vesicles (<100 nm) up to big ones with diameters larger than 1 μm. Most of the vesicles are cross-fractured, and the interlamellar distances can be determined to be about 600 Å. All space is filled with vesicles, especially gaps between bigger vesicles are filled with smaller ones. Thus, mechanical strain has to deform bilayers, which interact strongly due to their electrostatic repulsion. This gives an indication of where the elastic properties and the yield stress value of this densely packed vesicle system originate from. Another interesting feature is the encapsulation of small vesicles within the bigger ones.

If this vesicle solution is sheared for 1.5 h at a shear rate of 200 s^{-1} and then quenched in liquid propane immediately after the shearing has been stopped, a totaly different situation is observed (Figure 7a). The vesicles are now much smaller (500 nm and smaller) and the size polydispersity is reduced. The vesicles are oligolamellar, and the upper limit of the shell number is 5 or 6, whereas there had been more than 10 shells in the unsheared system. The space in the sheared system is not filled completely with vesicles, because there are many unilamellar vesicles that are smaller than the interlamellar distance in the unsheared system. The bigger vesicles in the sheared system are elongated and deformed due to the shear forces, while the small vesicles exhibit quite a round shape. Many larger vesicles are caught in an intermediate situation where the stripping and budding process is caught by the cryofixation.

Figure 7b displays the situation at a shear rate of 2000 s^{-1}. The vesicle size is decreased further to sizes as small as 100 nm or even smaller. The upper limit of vesicle shells is now four and the majority of the vesicles are unilamellar (in agreement with the conductivity data in III.2.1). The polydispersity is drastically reduced. There are still a few bigger vesicles that are elongated and deformed, while the unilamellar vesicles are perfectly round. It is likely that the bigger vesicles have still not found their ideal curvature and are thus prone to further change.

Increase of the shear rate up to 4000 s^{-1} (Figure 7c) leads to basically unilamellar vesicles of ca. 100 nm diameter. The occurrence of larger vesicles is very rare now. No more than two shells are observed. Some vesicles show the interesting feature where the actual ripping off of the outer (second) vesicle shell has been caught by TEM. Also, the asymmetric position of the second shell relative to the inner shell is displayed. This

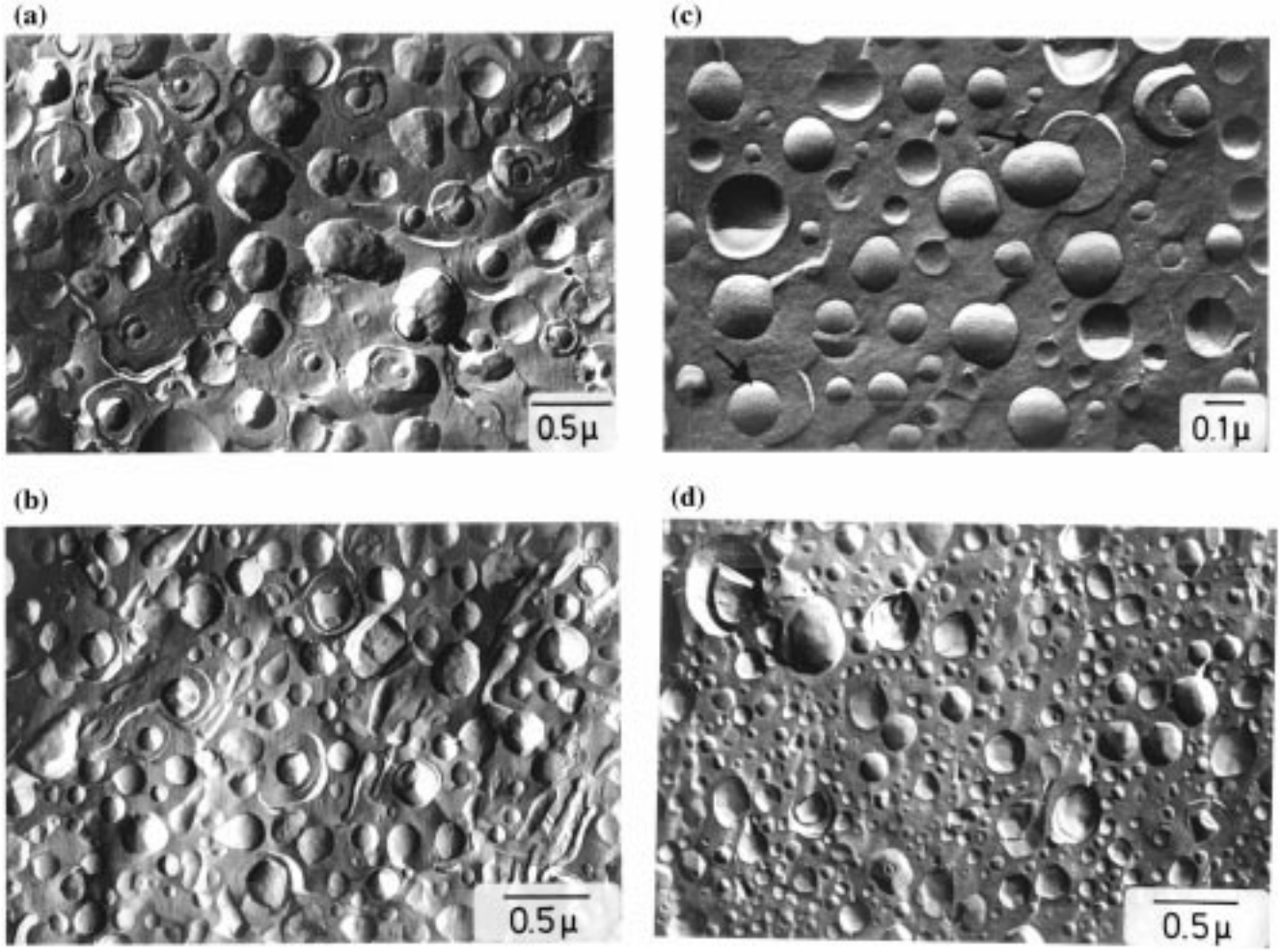

Figure 7. FF-TEM micrographs of the system 90 mM TDMAO/10 mM TTABr/220 mM 1-hexanol: (a) immediately after shearing the sample for 1.5 h at a shear rate of 200 s^{-1}; (b) at a shear rate of 2000 s^{-1}; (c) at a shear rate of 4000 s^{-1}; (d) after allowing the system to relax under stirring for 12 days.

is the state immediately before the ripping off of the second shell takes place.

To find out about the stability of the shear-imposed changes, a sample was freeze-fractured, which was allowed to stand for 12 days under stirring at room temperature after it had been sheared for 1.5 h at a shear rate of 2000 s^{-1} (Figure 7d). The micrograph reveals that in principle the same small and partly unilamellar vesicles as those cryofixed immediately after the shearing (Figure 7c) are present, and only a minor increase in the number of bigger, multilamellar vesicles is observed. The vesicles do not grow in size and do not build up a multilamellar structure of the 'onion' type, as was found before the shearing (Figure 4d). After stopping the shear a very high storage modulus and a correspondingly high yield stress value are built up, which prevent the system from relaxing back to its original state (cf. III.2.2). Thus, the state immediately after the shearing is fixed and kept over long periods of time. By the shear a permanent change was imposed on the system. Shearing a vesicle solution is therefore a proper tool to control the size of vesicles and to reduce the polydispersity.

III.2.4. Small-Angle Neutron Scattering (SANS). To monitor the structural changes that occur during the shear process in more detail, we performed SANS experiments in a Couette shear cell.[23] The q range was chosen in such a way as to cover well the interaction peak that is observed in the unsheared sample at $q = 0.0112$ 1/Å. This interaction peak is due to the multilamellar structure of the vesicles present and corresponds to a mean interlamellar spacing of 560 Å, a value that agrees well with the electronmicrographs (Figure 4d).

In Figure 8a, the radially averaged scattering intensity is given for various shear rates. To achieve a steady-state condition, an equilibration time of more than 1 h at the given shear rate was allowed prior to the measurement. Application of shear leads to a decrease of the peak intensity that is already largely diminished for a shear rate of 200 s^{-1} and disappears completely for shear rates above 1000 s^{-1}. This confirms nicely the result from electronmicroscopy; that is, the shells of the multilamellar vesicles are stripped off and the interaction peak disappears when basically no more multilamellar vesicles are present. In addition, it is interesting to note that at still higher shear rates a broad and only little pronounced peak starts to appear at much lower q. For the highest shear rate, its position is at $q = 0.006\,35$ 1/Å. Assuming this to be the interaction peak due to the interparticle interference of the newly formed unilamellar vesicles, this corresponds to a mean distance of 1000 Å between neighboring vesicles. This should also be the mean particle diameter for a densely packed system and is again in very good agreement with the electronmicrographs (see parts c and d of Figure 7).

In a next step, we looked at the relaxation process that takes place after switching off the shear. For this, the shear was stopped abruptly after having sheared for more than 2 h at 6000 s^{-1} and SANS curves were recorded in time intervals of 3 min in the beginning and increasingly longer times after 1 h had

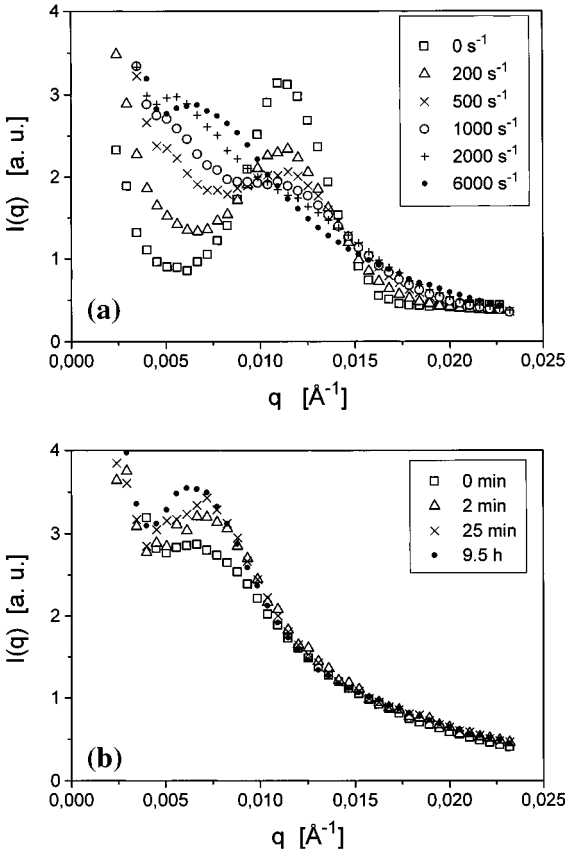

Figure 8. (a) Radially averaged SANS scattering intensity of the system 90 mM TDMAO/10 mM TTABr/220 mM 1-hexanol as a function of the scattering vector **q** for various shear rates. (b) SANS intensity curves for the relaxation process of the system 90 mM TDMAO/10 mM TTABr/220 mM 1-hexanol after switching off the shear gradient. The solution had been sheared previously for more than 2 h at 6000 s^{-1}.

passed (the measurement is bascially continuous; therefore, we assigned the meantime to a given curve). Some of the obtained intensity curves are given in Figure 8b, and it is evident that a relatively fast relaxation takes place in the first 30 min. Afterward, only fairly small further changes are observed. During this relaxation process, the rather weak peak that is visible during shear becomes more prominent but its position remains unaltered. This can be interpreted in a way that during the relaxation process the size of the unilamellar vesicles remains constant but their degree of ordering increases. The system relaxes from a highly disordered state that is present under shear to one where the vesicles possess a higher degree of positional ordering. This increase in positional ordering should be accompanied also by a higher degree of monodispersity of the vesicles, since a high degree of monodispersity has to be present in order to observe a more pronounced particle−particle interaction peak.

All the evidence from the effect of shear on macroscopic properties (shear modulus and conductivity) and on microscopic, structure-sensitive properties (FF-TEM and SANS) shows unambiguously that under shear vesicle shells are ripped off until at high shear rates unilamellar vesicles are formed. The stripping off of the vesicle layers seems to be the only process that is responsible for the behavior of vesicles under shear. This can be seen in Figure 9. Here, a shear rate of 200 s^{-1} has been applied and the change of both the conductivity (a macroscopic property) and the intensity of the Bragg scattering peak (a structure-sensitive, microscopic property) are observed with evolving time after turning on the shear.

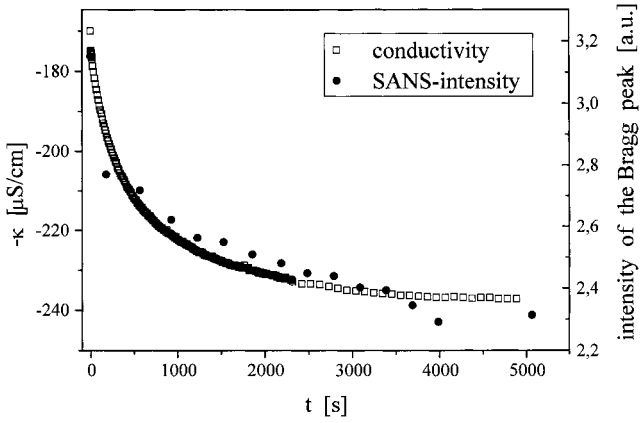

Figure 9. Plot of specific conductivity κ and Bragg peak intensity versus evolving time when a constant shear rate of 200 s^{-1} is applied for a sample of 90 mM TDMAO/10 mM TTABr/220 mM 1-hexanol/water.

Both conductivity and scattering intensity are affected in an exponential way and on the same time scale. This is to be expected, because the conductivity is proportional to the number of released counterions and thus the number of stripped off vesicle shells. The intensity of the Bragg peak depends on the number of vesicle shells within the vesicle, and its decrease is proportional to the number of stripped off vesicle shells. But, if both macroscopic properties such as the conductivity under shear (also the apparent shear viscosity scales on the same time scale as the Bragg peak, not shown) and microscopic, structure-sensitive quantities such as the Bragg scattering peak behave and scale in the same way, only one process can be responsible for the obtained results, the stripping off of vesicle shells. No second process (deformation or orientation processes could be imagined) is of any significance.

With all the evidence from conductivity, rheological, FF-TEM, and SANS experiments, we have clearly demonstrated that the multilamellar vesicles that are formed spontaneously in our system can be transformed by shear to unilamellar vesicles. This occurs by consecutive stripping off of the outer shells and is more pronounced the higher the shear rate. This resembles results of shear experiments done by Roux et al. on lamellar phases that are transformed to multilamellar vesicles, where also a decrease of vesicle size with increasing shear rate was observed.[38] However, our experiments are different insofar as we already started from a vesicle state and arrive at a state of monodisperse unilamellar vesicles (whereas in ref 35 the multilamellar vesicles do not become unilamellar but instead another transformation to ordered planar lamellar structures is observed). Therefore, the situation in our case is principally different and is the first case where the formation of unilamellar vesicles induced by shear is observed. After the shear has been turned off, our system remains permanently altered and the formed unilamellar vesicles are much more monodisperse than the original vesicles. This shows that the state of these vesicle system can be well-controlled by the application of a shear field.

III.3. Behavior of Lamellar Phases under Shear That Contain 0−10 mol % TTABr. As already argued from the TEM micrographs (Figure 4), the main difference between the highly charged (10 mol % TTABr) and the low charged vesicle phase (0.25−1 mol % TTABr) is the fraction of planar lamellar fragments still present in the low charged vesicle phase. This is to be expected because one starts from a lamellar phase of stacked bilayers (for no TTABr present) and finally reaches the 'onion' phase upon charging up the lamellae by stepwise addition of the cationic surfactant TTABr (as is the case for

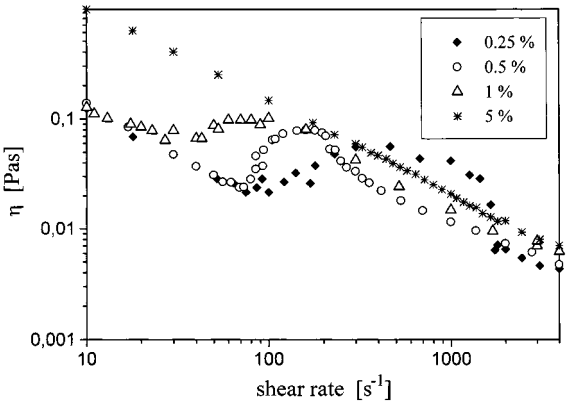

Figure 10. Double log plot of the apparent shear viscosity η versus the shear rate for different degrees of content of ionic surfactant (0.25, 0.5, 1, 5 mol % TTABr).

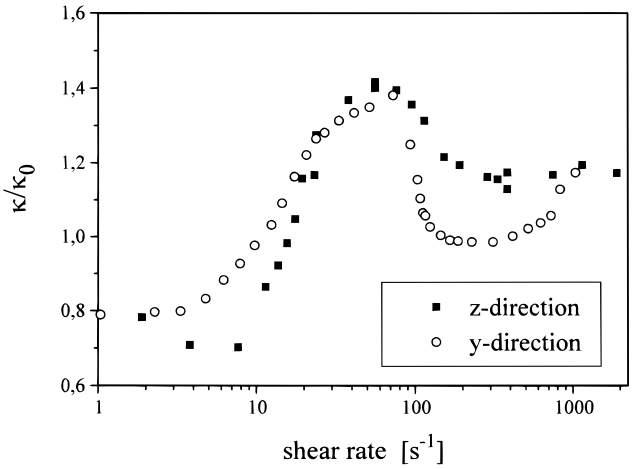

Figure 11. Plot of the reduced conductivity κ/κ_0 versus the shear rate for different directions (y and z) and a sample of composition 99 mM TDMAO/1 mM TTABr/220 mM 1-hexanol (1 mol % TTABr).

10% TTABr present). In the following, we will study systematically the effect of having increasing amounts of lamellar fragments present by reducing the charge density of our system and all samples will have the following composition: 100 mM (TDMAO/ TTABr)/220 mM 1-hexanol/water.

III.3.1. Rheology. Figure 10 shows a plot of the apparent viscosity under shear versus the shear rate for different contents of TTABr. The viscosity was measured with increasing shear rate. Each shear rate was held until a stationary value of the shear viscosity was obtained, which no longer changed with evolving time. This was usually the case after a equilibration time of 2−3 h. The vesicle solution that was charged up by the presence of 5 mol % TTABr (no lamellae present) shows the typical shear thinning behavior in the double logarithmic plot. Such a shear thinning is already expected for a relatively densely packed dispersion of hard spheres (which should be a simplified description of our vesicle system)[39] and has similarly been observed for unilamellar phospholipid vesicles.[35] The slope in the double logarithmic plot is −0.85 (Figure 10) and therefore significantly larger than the value of −0.57 that has been observed in the case of the phospholipid vesicles.[35] This is reasonable since in the latter case no structural transformation of the vesicles has been reported, whereas in our case vesicle shells are stripped off, and evidently this leads to a more pronounced shear thinning effect. The sample containing 10 mol % TTABr shows a very similar rheological behavior and has therefore been omitted in Figure 10. It should also be noted that the samples containing only large multilamellar vesicles, i.e., for 5 and 10 mol % TTABr, have a much higher zero-shear viscosity due to the dense packing of the vesicles in this system.

The solutions with small charge density (0.25−1 mol %) also show shear thinning behavior in general, but here a region of shear thickening is also observed. Evidently, here some more complex structural transition takes place. Its position and pronouncedness depend on the charge density. The higher the charge density the more it is shifted to lower shear rates (from 600 s^{-1} (0.25%) via 150 s^{-1} (0.5%) down to 70 s^{-1} (1%)) and the less pronounced it is. The sample with pure TDMAO is not included in Figure 10 since its viscosity becomes readily too low to be measured under identical conditions, which is due to the fact that this sample is made up purely of planar lamellae. It is interesting to note that apparently under the given shear conditions no vesicles are formed in the pure TDMAO system.

This shear thickening behavior can be explained by a structural transformation of the lamellae into vesicles, because the formed vesicles have a higher viscosity than the planar lamellae. For the system charged up by the presence of 0.25 mol % TTABr, the fraction of planar lamellae is the highest. Thus, the maximum is the broadest, because more energy is needed to transform all the lamellae into vesicles. On the other hand, the critical shear rate for the transformation of this system is the highest because the tendency for formation of vesicles is the lowest due to its small charge density (since the Gaussian modulus $\bar{\kappa}$ of the bilayer becomes more negative with increasing charge density, and a more negative $\bar{\kappa}$ will favor vesicle formation[9,32]). Thus, higher shear rates are needed to transform the bilayer into highly curved vesicles. On passing the maximum (and thus the point of structural transition), the viscosity shows shear thinning behavior again, because the formed vesicles decrease in size, due to the stripping off of vesicle shells.

The regime of the viscosity maximum is accompanied by extremely long equilibration times (more than 3 h), and the viscosity values are somewhat noisy. This favors the idea of a structural change that needs time to develop, i.e., is dominated by slow kinetics. If the viscosity is measured first with increasing and then with decreasing shear rate, one finds hysteresis curves (not shown), where the hysteresis effect is larger the shorter the equilibration time at a given shear rate. At the same time, the viscosity maximum for the samples of low TTABr content gets the more pronounced the longer time the system is given to adjust to a certain shear rate. This indicates that the transformations need different times for their buildup and their decay. These structural changes are obviously not readily reversible (on experimental time scales), because the measurement of the shear viscosity with decreasing shear rate yields different viscosity values, even for equilibration times of several hours.

III.3.2. Electric Conductivity. Figure 11 shows a plot of the reduced conductivity κ/κ_0 (κ conductivity under shear, κ_0 conductivity at rest without shearing) versus the shear rate for a sample that contains 1 mol % TTABr. With increasing shear rate, the conductivity in both the flow and the vorticity direction rises due to the preferred parallel orientation of lamellar sheets (cf. SANS experiments, III.3.3; orientation of the lamellae will always be denoted as follows: parallel for the lamallar director along the velocity gradient; perpendicular for the lamellar director along the vorticity direction; transpose for the lamellar director along the flow direction) until at a shear rate of 70 s^{-1}, a maximum, is reached. The position of this maximum corresponds exactly to the onset of the shear thickening found in rheology (see Figure 9).

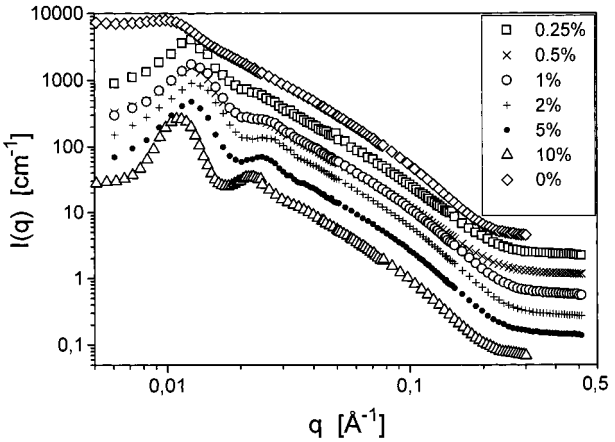

Figure 12. Radially averaged SANS curves at rest for the variously charged samples in the system 100 mM (TDMAO/ TTABr)/1-hexanol/ D_2O at 25 °C. The amount of TTABr in the surfactant mixture is given in mol %. $I(q)$ is valid for 10%; subsequent curves were each multiplied by a factor of 2.

At this point, the transformation of planar lamellae into vesicles begins, which leads to a marked decrease of the conductivity in both directions due to the entrapment of counterions. This decrease of conductivity is, of course, isotropic and found for both the flow and the vorticity direction at exactly the same shear rate. After the minimum toward higher shear rates, the conductivity in the vorticity direction is basically constant while it increases significantly in the flow direction. This increase may be ascribed to the deformation of vesicles along the flow direction, which should lead to an increase of conductivity in the flow direction and a concomitant decrease in the vorticity direction. Such a decrease is not observed, but this is presumably due to the fact that at the same time at higher shear rates from the large multilamellar vesicles shells are stripped off, which will lead to an overall increase in conductivity (as described in III.2).

It is also noteworthy that upon starting the shear a fast drop of the conductivity is observed in the vorticity direction, which can be explained by orientation effects of the planar lamellae (see also III.3.3); that is, here lamellar sheets that, due to the filling process, were originally oriented transpose are quickly reoriented parallel and perpendicular.

III.3.3. Small-Angle Neutron Scattering (SANS). To obtain more detailed information regarding the structural changes that occur in these lamellar phases, SANS measurements in a Couette shear cell were performed on samples that contained 0.25, 0.5, and 1 mol % TTABr. Again, in all cases we allowed for equilibration times of about 1 h at a given shear rate. In additon, samples containing 0, 0.25, 0.5, 1.0, 3.0, 5.0, and 10.0 mol % TTABr were investigated at rest in cuvettes.

III.3.3.1. Samples at Rest. In Figure 12, the radially averaged intensities are given for the differently charged samples at rest. In all cases, a lamellar peak is observed that becomes more pronounced with increasing TTABr content and in particular the second-order peak becomes more pronounced. For the uncharged sample, the lamellar peak is only weakly visible. This means that the degree of order increases with increasing charge density of the bilayers due to the electrostatic repulsion. The peak position q_{max} moves with increasing charge density, first to higher q values and then, for samples with more than 3% TTABr, to lower values again. The corresponding interlamellar spacings d (as calculated from $d = 2\pi/q_{max}$) are given in Table 1.

TABLE 1: Interlamellar Spacing *d*, and Lamellar Thickness *D* for the Samples Composed of 100 mM (TDMAO/TTABr)/ 220 mM 1-hexanol/D_2O for the Variously Charged Systems As Obtained from the SANS Curves

mol % TTABr	0	0.25	0.5	1.0	3.0	5.0	10.0
d (Å)	631	507	498	492	489	501	563
D (Å)	24.3	20.5	19.9	20.8	20.9	22.2	24.5
d/*D*	26.0	24.8	25.0	23.7	23.4	22.6	22.9

In addition, we determined the lamellar thickness D (for SANS the lamellae contain alkyl chains and headgroups of the surfactant) from the high q part of the scattering curves. Well beyond the correlation peak, the scattering curve should be given by the scattering law of individual lamellae. The scattering law for homogeneous flat lamellae of thickness D is given by[40]

$$I(q) = \frac{2\pi}{q^2}\Phi_L \Delta\rho^2 D\left(\frac{\sin(qD/2)}{(qD/2)}\right)^2 \qquad (2)$$

with $q = (4\pi/\lambda)\sin(\theta/2)$, λ = wavelength of the neutrons, θ = scattering angle, $\Delta\rho$ = difference of the scattering length densities of solvent and lamellae, and Φ_L = volume fraction of the lamellae.

With this expression, the SANS curves were fitted for the range $q > 0.04$ 1/Å, i.e., well beyond the interaction peak. The obtained lamellar thickness D is given in Table 1. It is interesting to note that D follows the same trend as the interlamellar spacing d. With increasing charge density it first decreases and then becomes larger again.

For the change of d with increasing content of TTABr, two effects have to be considered. First, the increasing electrostatic repulsion of the bilayers should lead to a decrease of the mean spacing between the bilayers. A good measure for this effect should be the ratio d/D, which is a 'normalized spacing'. It is given in Table 1 and decreases continuously with increasing charge density of the amphiphilic bilayer. Therefore, clearly this effect seems to be of importance in our system. The second effect is that it has been shown above that with increasing content of TTABr a transformation of lamellar sheets into vesicles takes place. However, due to the lower effective packing fraction of the bilayers in the vesicles the mean spacing in multilamellar vesicles has to be smaller than that in the planar lamellar phase, the more so the lower the number of vesicle shells. Both these effects explain our experimentally observed trends, since both electrostatic repulsion and transformation of planar lamellae into vesicles will lead to a decrease of d. However, this effect is counterbalanced at higher TTABr content, since here the number of shells grows considerably (as evidenced by the electronmicrographs; Figure 4) thereby increasing the mean spacing d again.

III.3.3.2. Experiments under Shear. When the samples are sheared, this peak rapidly disappears in all cases, as is shown in Figure 13. One also observes that for the samples of low TTABr content the overall scattering intensity increases after the shear is turned on. This effect is very pronounced for the 0.25 mol % TTABr sample and becomes less pronounced with increasing concentration of TTABr. This can be explained by the fact that at low TTABr content a large amount of the amphiphilic material is present in the form of lamellar fragments. However, these will largely become oriented parallel during the filling process, which means that they contribute less to the scattering intensity. Once the shear is turned on, the lamellar fragments start to become reoriented and at higher shear rates are transformed into vesicles, which means that now more of the bilayer is oriented parallel to the incident beam and contributes more strongly to the scattering intensity.

For the samples with high content of TTABr already at rest, all the bilayers are present in the form of vesicles and therefore this effect is not observed at all (cf. III.2.4). It may be noted that the thickness of the bilayer (determined by analysis of the high q region by means of eq 2) is not affected at all by the presence of the shear gradient. It should also be noted that for all the systems studied (also for the 10% TTABr sample, cf. Figure 8a) the peak position, q_{max}, is not significantly changed by the shear. This is different from the observation of Roux et al. where an increase of q_{max} with rising shear rate has been found that has been interpreted by an expulsion of water from the intermembrane space.[41] No such effect seems to occur in our system.

For the sample containing 0.25 mol % TTABr, one observes that the scattering pattern is drastically changed upon turning on the shear but then remains unaltered in the range of shear rates of 20−1000 s^{-1} (Figure 13a) and still shows the indication of an interlamellar peak around 0.0125 1/Å. For the higher shear rates of 2000 and 6000 s^{-1}, some increase of the scattering intensity in the low q range is observed and the peak becomes somewhat less pronounced. Insofar the behavior is similar to that of the 10% sample, but there, these changes occurred at much lower shear rates (cf. III.2.4). This can be explained in such a way that in the 0.25 mol % sample, which originally contained large amounts of lamellar fragments, a transformation of these lamellar fragments into multilamellar structures is induced by the presence of the shear field up to fairly high shear rates. Only at the highest shear rates then the 'stripping process' sets in that reduces the number of shells of the multilamellar vesicles.

The samples with 0.5% and 1% TTABr behave similarly, with the difference that the effect of the highest shear rate (6000 s^{-1}) now becomes more pronounced. This means that here this highest shear rate is more effective in reducing the number of shells of the multilamellar vesicles. But contrary to the 10% sample, even this fairly high shear rate is not yet sufficient to strip off all the shells and give rise to the formation of the small unilamellar vesicles. This means that the less charged the system the more resistant it is to the mechanical stress caused by the shear field. But this also means that our system can support better a highly curved bilayer (as present in the small unilamellar vesicles) the more highly charged the bilayer; that is, we observe a tendency for formation of more highly curved interfaces with increasing charge density.

III.3.3.3. Time-Dependent Changes under Shear. The scattering pattern of these samples is not radially symmetric, but due to the shear field, anisotropy is to be expected. This can be seen in Figure 14, which depicts the effect of shear on the sample containing 0.25 mol % TTABr. Prior to shear, a peak is seen in the horizontal (which means that the lamellae are preferentially oriented transpose, parallel orientation is not visible in this experiment), as a result of the filling process of the Couette cell. Immediately after the shear is turned on, this peak is flipped into the vertical direction, which is clear since a transpose orientation of the lamellae is the most unstable in the shear field. At the beginning, this vertical peak is fairly pronounced but becomes less pronounced with evolving time. However, the lobes in the vertical direction (which are due to perpendicular lamellar sheets) remain present even after more than 1 h and are not completely transferred to other orientations. Therefore, this perpendicular orientation is not an artifact due to the filling process (which produced some transpose lamellar) but is a real effect. Further experiments on similar systems where SANS experiments were done both in the perpedicular and tagential directions with respect to the Couette cell corroborate the stability of the perpendicular orientation under the given conditions.[42]

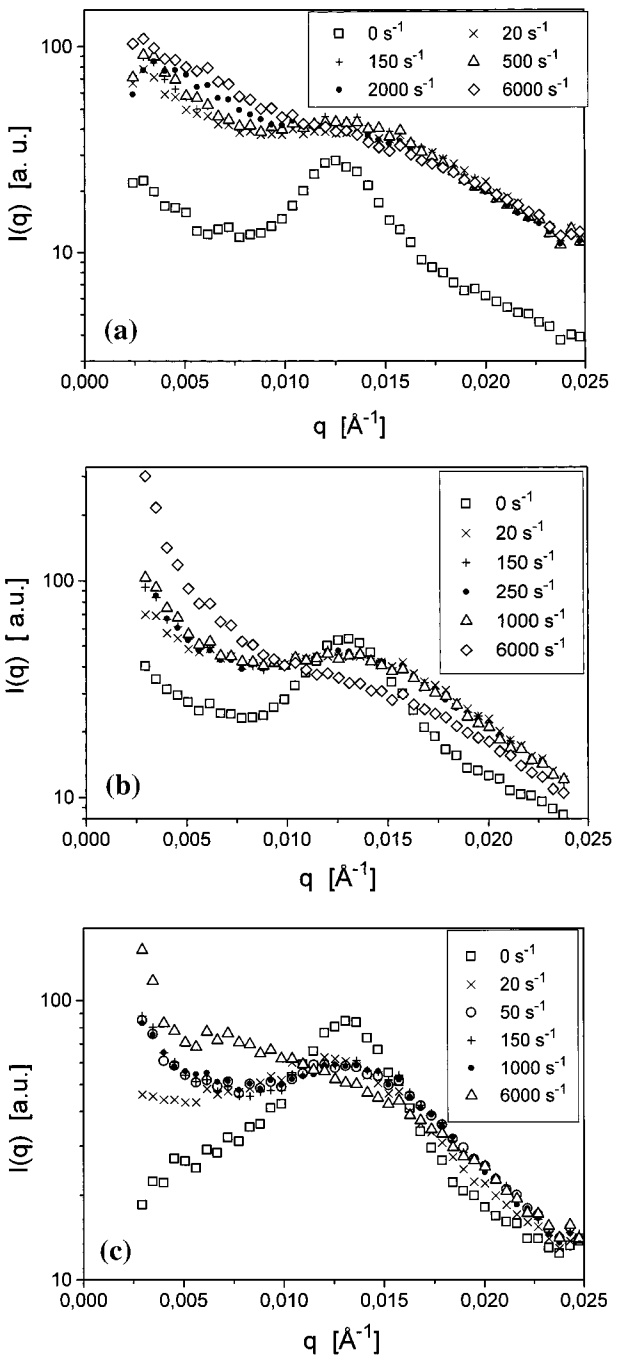

Figure 13. Radially averaged SANS curves for various shear rates for samples containing (a) 0.25 mol % TTABr, (b) 0.5 mol % TTABr, (c) 1.0 mol % TTABr.

At the highest shear rate of 6000 s^{-1}, these lobes have disappeared but still a markedly anisotropic scattering pattern is observed. This should be due to the deformation of the formed vesicles, and the ellipsoidal anisotropy observed in Figure 14d should correspond to the ellipsoidal deformation of the vesicles. A similar behavior as a function of the shear has been observed for the other samples investigated in the shear cell (0.5 and 1 mol % TTABr).

A good way to analyze the effect of shear on the scattering curves is by looking at the azimuthal dependence of the scattering intensity. This is shown for the sample containing

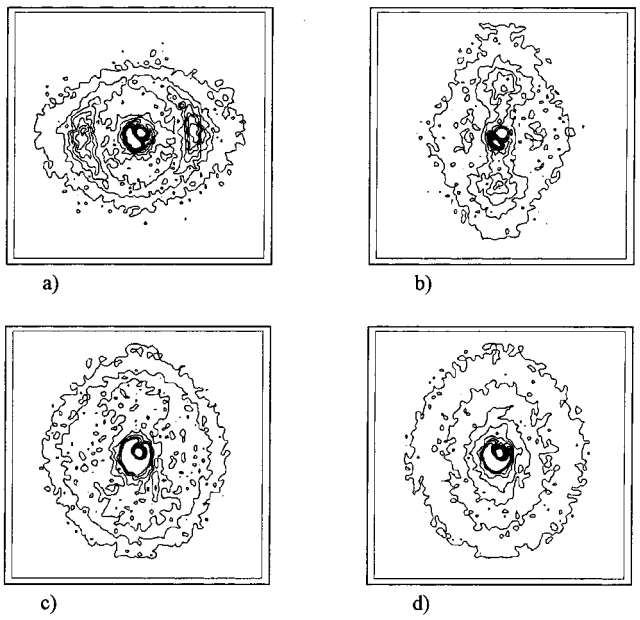

Figure 14. Contour plot of the two-dimensionally detected scattering intensities for a sample of 99.75 mM TDMAO/0.25 mM TTABr/220 mM 1-hexanol in D_2O at various stages of the shear experiment (the detector corresponds to the $y-z$ plane with y (flow direction) being the horizontal and z (vorticity direction) the vertical axis in the contour plots): (a) at rest; (b) immediately after turning on a shear rate of 20 s^{-1}; (c) after a shear rate of 20 s^{-1} had been applied for about 1 h; (d) at a shear rate of 6000 s^{-1} after 1 h.

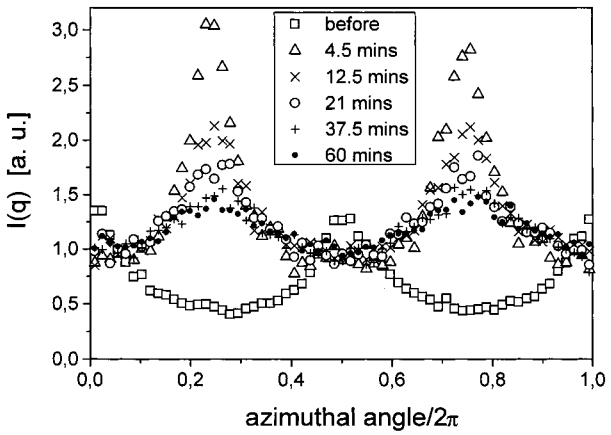

Figure 15. Circularly averaged SANS curves for the sample of 99.75 mM TDMAO/0.25 mM TTABr/220 mM 1-hexanol in D_2O at various stages of the shear experiment for the experiment where at $t = 0$ a shear rate of 20 s^{-1} has been switched on.

0.25 mol % TTABr in Figure 15 for various stages of the shear experiment. It is evident that immediately after the shear is turned on the anisotropy of the scattering pattern becomes very pronounced, but this anisotropy relaxes as a function of time. This is shown in Figure 16 for the case of the 0.25 mol % TTABr sample and the shear rate of 20 s^{-1}. The anisotropy factor is defined as the ratio between the maximum and minimum intensity of the circularly averaged scattering intensity. The relaxation of the anisotropy and that of the intensity of the Bragg peak take place at the same rate (which means that both processes are coupled to the same structural changes).

For the case shown here, one observes a relaxation time of about 9 min. This relaxation time increases with increasing charge density to 12 min for the 0.5 mol % TTABr sample and to 32 min for the 1 mol % TTABr sample. This means that the time for structural equilibration in the shear field increases with

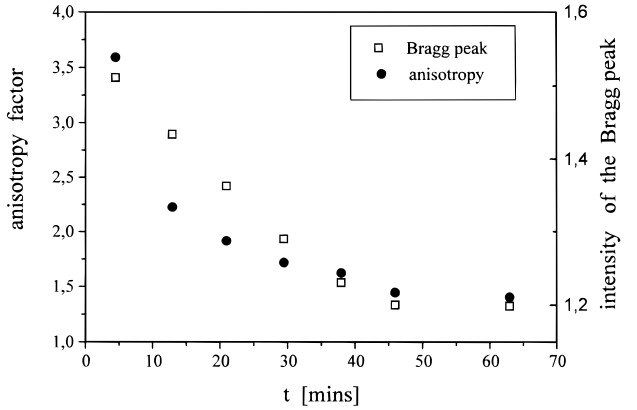

Figure 16. Anisotropy factor and intensity of the Bragg peak as a function of evolving time after turning on a shear rate of 20 s^{-1} for a sample of 99.75 mM TDMAO/0.25 mM TTABr/220 mM 1-hexanol in D_2O.

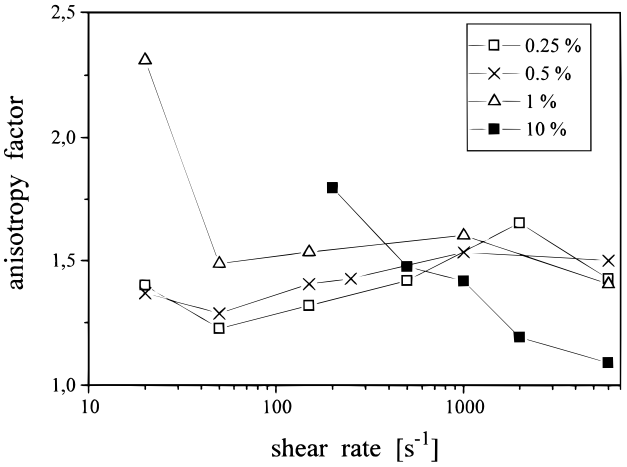

Figure 17. Anisotropy factor for the variously charged systems as a function of the shear rate (always taken at the end of the equilibration time of 1 h per measurement). The molar percentage of TTABr is indicated.

increasing charge density of the system. The process monitored here should correspond to a reorientation of lamellar sheets that at the beginning are oriented perpendicularly and then flipped into the parallel orientation that seems to be the more stable orientation. This process requires longer times with increasing content of ionic TTABr. This may be explained by the fact that for the reorientation process lamellar fragments have to change their relative position to each other and this movement will be more hindered with increasing electrostatic repulsion between the lamellae.

Another interesting comparison of the behavior of the differently charged systems in the shear field can be done if one considers the anisotropy factor that is observed at the end of the equilibration time at a given shear rate. These values are compared in Figure 17 for samples containing 0.25, 0.5, 1, and 10 mol % TTABr. One observes that for the samples of lower charge density (0.25 and 0.5 mol % TTABr) an increase of the anisotropy is observed with rising shear rate and only at the highest shear rate it becomes smaller again. For the 1% sample, almost constant values are found, and for the 10% sample, a continuous decrease is observed.

This can be explained in such a way that for the anisotropy two opposing effects are present. First lamellar fragments are transformed into multilamellar vesicles. These large multilamellar vesicles become deformed by the shear field, and this is seen increasingly so with rising shear rate (thereby increasing

the anisotropy factor). This is what is observed for the samples of low TTABr content, which originally contain large amounts of planar lamellae. The other effect is the 'stripping process', where the large multilamellar vesicles loose their shells and in the end are transformed into small unilamellar vesicles. Of course, the smaller the vesicles the less they will be deformed and thereby the anisotropy factor becomes smaller. This then is the case for the highly charged samples and explains why here the anisotropy decreases with increasing shear rate, since one already starts from the situation of large multilamellar vesicles that only become smaller during the shear process. This effect of reducing the size of the vesicles is, for the samples containing 0.25 and 0.5 mol % TTABr, only observed at the highest shear rate (in agreement with the radially averaged intensity changes; cf. Figure 13).

To summarize, we can state that one observes four different effects during the shear process. Originally, one has a preferential orientation of the lamellae in the vorticity direction due to the filling process (causes the horizontal SANS peak). Immediately after turning on the shear, one finds a flip of the lamellar sheets with transpose orientation to perpendicular and parallel (pseudoisotropic) orientation (causes the SANS peak in the vertical). In a next step, the perpendicular lamallar fragments will more slowly become reoriented into the more stable parallel orientation, which reduces the anisotropy of the scattering pattern. That such an orientation, is often the most stable one for not too high shear rates has also recently been demonstrated experimentally for the planar lamellar phase of a nonionic surfactant.[43] Similar orientational effects have also been observed for a defective lamellar phase in the ionic system SDS/decanol, where for lower shear rates parallel orientation has been found that changes to perpendicular orientation with increasing shear rate.[44]

A third effect is that the lamellar fragments can become transformed into multilamellar vesicles. These larger vesicles are now more easily deformed, which leads again to preferred anisotropy in the vorticity direction and is opposite to the effect mentioned before with respect to the anisotropy observed. Finally, the large multilamellar vesicles are reduced in size at high shear rates and the smaller vesicles formed are less deformed in the shear field and this will reduce the observed anisotropy again. It should be noted that the last two effects involve structural transformation and will reach a steady state at a given shear rate that takes considerable time to be reached.

III.3.4. Freeze−Fracture Transmission Electron Microscopy (FF-TEM). Figure 18 displays a FF-TEM micrograph of a sample that is charged up by the presence of 0.25 mol % TTABr. It has been sheared for 4 h at a shear rate of 400 s^{-1} (in the regime of the rheological maximum; see Figure 10). Then, it has been quenched in liquid propane and freeze-fractured. As can be seen that the situation is completely different from the one in the unsheared state (see Figure 4a). Extended lamellar sheets are no longer observed. The basic structure is vesicular. The size range is from 30 up nm to around 300 nm (it might be noted that they are still significantly smaller than the vesicles observed in the 10 mol % TTABr system). This demonstrates that the effect of the presence of the shear field has been a transformation of planar lamellae into vesicles.

The micrograph reveals many dynamic processes. In the center of the picture an elongated, tubular particle can be noted that wraps around a vesicle. Many wormlike tubuli are present with a preferential orientation from the bottom to the top of the picture. This orientation may result from the shearing in the Couette cell but may also be introduced artificially by the freeze−fracture preparation process. Many vesicles are deformed and obviously not in an equilibrium situation. There are small lamellar fragments 'floating' around that are not yet transformed into vesicles. Thus, the micrograph indicates that there is a structural transformation going on. Looking at this picture, it is easily understood that the rheological equilibration time is extremely long and that obtained apparent shear viscosity data are a little noisy in the regime of the structural transition from planar lamellae to vesicles.

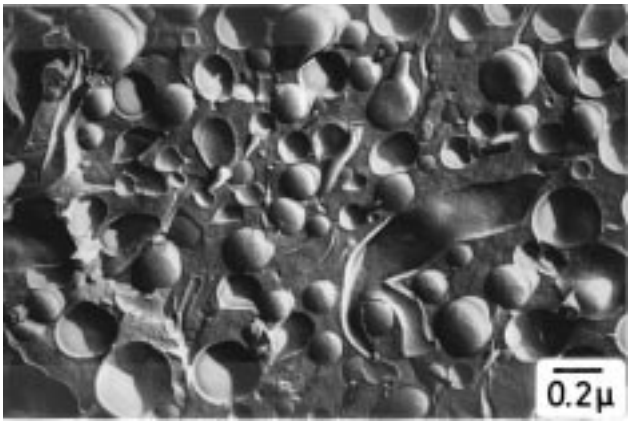

Figure 18. FF-TEM micrograph of a sample that is charged up by the presence of 0.25 mol % TTABr and that had been sheared for 4 h at a shear rate of 400 s^{-1}. Then, it was quenched immediately in liquid propane and freeze-fractured.

IV. Conclusions

The influence of shear on the properties and structure of a bilayer system has been studied as a function of the charge density of the surfactant system by means of various methods (rheology, electric conductivity in the shear field, SANS, FF-TEM). The charge density was controlled by the amount of cationic surfactant (TTABr) that was present in a mixture with a nonionic surfactant (TDMAO) where the surfactant mixture was always of a constant concentration of 100 mM. Investigations of the systems at rest showed that systems with more than 3 mol % cationic surfactant contain multilamellar vesicles, whereas at lower charge density, increasing amounts of planar lamellae are present in equilibrium with multilamellar vesicles.

For the samples containing a mixture of planar lamellar fragments and multilamellar vesicles, the influence of shear leads to a transformation of these lamellae into multilamellar vesicles, as evidenced by the FF-TEM and the SANS experiments. The region of shear rates where this transformation takes place is accompanied by an increase in viscosity, i.e., a shear thickening, due to the formation of large multilamellar structures. The critical shear rate of this transition of planar lamellae into vesicles depends on the charge density of the system. The critical shear rate is smaller for solutions that contain more ionic surfactant (e.g., 1% TTABr). Here, the tendency for vesicle formation is higher. Such a system then needs a smaller impetus by shear to build up vesicles than a system with smaller spontaneous tendency (e.g., 0.25% TTABr).

These multilamellar structures are now themselves sensitive to shear, since their outer shells can become 'stripped off' due to the shear forces. For the low charged systems, one first observes formation of the multilamellar structures, and only at the highest shear rates their size becomes reduced again (as evidenced by the SANS pattern, especially its anisotropy). For the more highly charged systems, where one already starts from a situation where only multilamellar vesicles are present, this

effect is seen already at much lower shear rates. Here, the vesicles become continuously smaller with increasing shear rate and it is even possible to form small unilamellar vesicles at the highest shear rate. This means that it becomes easier to form small vesicles of higher curvature with increasing charge density of the amphiphilic bilayer.

Depending on the charge density of the system, a variety of different bilayer structures, i.e., vesicles and planar lamellae, can be formed in the pure or mixed state. By application of shear forces a transition into vesicle structures can be induced, and the size of these vesicles can be controlled by the shear rate employed. Therefore, one is able to control the structure and size of this bilayer system by carefully adjusting the charge density of the system and exposing the system for a sufficient time to a given shear rate.

Acknowledgment. We thank the TMR program of the European Community for financial support of the neutron scattering experiments at Risø National Laboratory through the large installation program. Also, we thank C. Thunig for help with the determination of the phase behavior and K. Sattler for help with the SANS experiments. Furthermore, we are grateful for financial support of this research project by the BMBF-Verbundprojekt VB42, Grant 03-H04BAY. Finally, we also thank the two anonymous reviewers for a number of helpful suggestions.

References and Notes

(1) *Handbook of Biological Physics*; Lipowsky, R., Sackmann, E., Eds.; Elsevier: Amsterdam, 1995; Vol. 1.
(2) *Vesicles*; Rosoff, M., Ed.; Surfactant Science Series 62; Marcel Dekker, Inc.: New York, 1996.
(3) Lasic, D. D. *Angew. Chem.* **1994**, *106*, 1765.
(4) Vuillemard, J. C. *J. Microencapsulation* **1991**, *8*, 547.
(5) Carnie, S.; Israelachvili, J. N.; Pailthorpe, B. A. *Biochim. Biophys. Acta* **1979**, *554*, 340.
(6) Talmon, Y.; Evans, D. F.; Ninham, B. W. *Science* **1983**, *221*, 1047.
(7) Kaler, E. W.; Murthy, A. K.; Rodriguez, B. E.; Zasadzinski, J. A. N. *Science* **1989**, *245*, 1371.
(8) Cantu, L.; Corti, M.; Musolino, M.; Salina, P. *Prog. Colloid Polym. Sci.* **1991**, *84*, 21.
(9) Winterhalter, M.; Helfrich, W. *J. Phys. Chem.* **1992**, *96*, 327.
(10) Roux, D.; Nallet, F.; Diat, O. *Europhys. Lett.* **1993**, *24*, 53.
(11) Panizza, P.; Roux, D.; Vuillaume, V.; Lu, C.-Y. D.; Cates, M. E. *Langmuir* **1996**, *12*, 248.
(12) Laughlin, R. G.; Munyon, R. L.; Burns, J. L.; Coffindaffer, T. W.; Talmon, Y. *J. Phys. Chem.* **1992**, *96*, 374.
(13) Gulik-Krzywicki, T.; Dedieu, J. C.; Roux, D.; Degert, C.; Laversanne, R. *Langmuir* **1996**, *12*, 4668.
(14) Diat, O.; Roux, D.; Nallet, F. *Phys. Rev. E* **1995**, *51*, 3296.
(15) Lukaschek, M.; Müller, S.; Hansenhindl, A.; Grabowski, D. A.; Schmidt, C. *Colloid Polym. Sci.* **1996**, *274*, 1.
(16) Bergenholtz, J.; Wagner, N. J. *Langmuir* **1996**, *12*, 3122.
(17) Läuger, J.; Weigel, R.; Berger, K.; Hiltrop, K.; Richtering, W. *J. Colloid Interface Sci.* **1996**, *181*, 521.
(18) Mendes, E.; Narayanan, J.; Oda, R.; Kern, F.; Manohar, C.; Candau, S. J. *J. Phys. Chem.* **1997**, *101*, 2256.
(19) Weigel, R.; Läuger, J.; Richtering, W.; Lindner, P. *J. Phys. II (France)* **1996**, *6*, 529.
(20) Richtering, W. *Prog. Colloid Polym. Sci.* **1997**, *104*, 990.
(21) Bergmeier, M.; Hoffmann, H.; Thunig, C. *J. Phys. Chem. B* **1997**, *101*, 5767.
(22) Bergmeier, M.; Gradzielski, M.; Hoffmann, H.; Mortensen, K. *J. Phys. Chem. B* **1998**, *102*, 2837.
(23) Norden, B.; Elvingson, C.; Eriksson, T.; Kubista, M.; Sjöberg, B.; Takahashi, M.; Mortensen, K. *J. Mol. Biol.* **1990**, *216*, 223.
(24) Chen, S. H.; Lin, T. L. *Methods of Experimental Physics* **1987**, *23B*, 489.
(25) Hoffmann, H.; Munkert, U.; Thunig, C.; Valiente, M. *J. Colloid Interface Sci.* **1994**, *163*, 217.
(26) Hoffmann, H.; Thunig, C.; Schmiedel, P.; Munkert, U. *Faraday Discuss.* **1995**, *101*, 319.
(27) Hoffmann, H.; Thunig, C.; Schmiedel, P.; Munkert, U. *Il Nuovo Cimento* **1994**, *16D*, 1373.
(28) Hoffmann, H.; Thunig, C.; Schmiedel, P.; Munkert, U. *Langmuir* **1994**, *10*, 3972.
(29) Valiente, M.; Thunig, C.; Munkert, U.; Lenz, U.; Hoffmann, H. *J. Colloid Interface Sci.* **1993**, *160*, 39.
(30) Schomäcker, R.; Strey, R., *J. Phys. Chem.* **1994**, *98*, 3908.
(31) Oberdisse, J.; Couve, C.; Appell, J.; Berret, J. F.; Ligoure, C.; Porte, G. *Langmuir* **1996**, *12*, 1212.
(32) Helfrich, W. *J. Phys.: Condens. Matter* **1994**, *6*, A79.
(33) Generalova, E. V.; Kitaeva, E. L.; Nesrullaev, A. N.; Sonin, A. S. *Colloid J. USSR* **1990**, *52*, 828.
(34) Soubiran, L.; Coulon, C.; Sierro, P.; Roux, D. *Europhys. Lett.* **1995**, *31*, 243.
(35) de Haas, K. H.; Blom, C.; van den Ende, D.; Duits, M. H. G.; Haveman, B.; Mellema, J. *Langmuir* **1997**, *13*, 6658.
(36) Graessly, W. W. *Advances in Polymer Science*; Springer: New York, 1974; Vol. 16.
(37) Thurn, H.; Löbl, M.; Hoffmann, H. *J. Phys. Chem.* **1985**, *89*, 517.
(38) Diat, O.; Roux, D.; Nallet, F. *J. Phys. II* **1993**, *3*, 1427.
(39) van der Werff, J. C.; de Kruif, J. C. *J. Rheol.* **1989**, *33*, 421.
(40) Porod, G. In *Small-Angle X-ray Scattering*; Glatter, O., Kratky, O., Eds.; Academic Press: London, 1982.
(41) Diat, O.; Roux, D.; Nallet, F. *Phys. Rev. E* **1995**, *51*, 3296.
(42) Gradzielski, M.; Escalante, J.; Hoffmann, H.; Mortensen, K. In preparation.
(43) Penfold, J.; Staples, E.; Khan Lodhi, A.; Tucker, I.; Tiddy, G. J. T. *J. Phys. Chem. B* **1997**, *101*, 66.
(44) Berghausen, J.; Zipfel, J.; Lindner, P.; Richtering, W. *Europhys. Lett.* **1998**, *43*, 683.